Supporting Information (SI)

Combining the Furoxanylhydrazone Framework with Various Energetic Functionalities to Prepare New Insensitive Energetic Materials with a 3D-cube Layer Stacking

Jie Tang [a], Hongwei Yang[a], Hualin Xiong [a], Wei Hu[a], Caijin Lei[a] and Guangbin Cheng*[a]

School of Chemical Engineering, Nanjing University of Science and Technology
Nanjing 210094, P. R. China

Email: gcheng@mail.njust.edu.cn

Table of Contents

1 Experimental Section

General methods

^{1}H and ^{13}C NMR spectra were recorded on 500 MHz (Bruker AVANCE 500) nuclear magnetic resonance spectrometers operating at 500 and 125 MHz, respectively, by using either DMSO-d_6 or acetone-d_6 as the solvent and locking solvent unless otherwise stated. Chemical shifts in ^{1}H and ^{13}C NMR spectra are reported relative to DMSO. DSC was performed at a heating rate of 5 °C min^{-1} in closed Al containers with a nitrogen flow of 30 mL min^{-1} on an STD-Q600 instrument. Infrared (IR) spectra were recorded on a Perkin-Elmer Spectrum BX FT-IR equipped with an ATR unit at 25 °C. Impact sensitivity, friction sensitivity and electrostatic discharge sensitivity of samples are measured by using the standard BAM methods.

X-ray crystallography

The data were collected with a Bruker three-circle platform diffractometer equipped with a SMART APEX II CCD detector. A Kryo-Flex low-temperature device was used to keep the crystals at a constant 173(2) K during the data collection. The data collection and the initial unit cell refinement were performed by using APEX2 (v2010.3-0). Data reduction was performed by using SAINT (v7.68A) and XPREP (v2008/2). Corrections were applied for Lorentz, polarization, and absorption effects by using SADABS (v2008/1). The structure was solved and refined with the aid of the programs in the SHELXTL-plus (v2008/4) system of programs. The full-matrix least-squares refinement on F2 included atomic coordinates and anisotropic thermal parameters for all non-H atoms. The H atoms were included in a riding model. The structure was solved by direct methods with SHELXS-97 and expanded by using the Fourier technique. The nonhydrogen atoms were refined anisotropically. The hydrogen atoms were located and refined.

2 The Crystallographic Data

The crystal of **5**, **7**, **10**•H_2O, **11**•$3H_2O$ and cocrystal **8/4** were performed on a Bruker Smart Apex II diffractometer with graphite-monochromated Mo Kα radiation (λ= 0.71073 Å), respectively. Integration and scaling of intensity data were accomplished using the SAINT program2. The structures were solved by intrinsic using SHELXT2014 and refinement was carried out by a full- matrix least-squares technique using SHELXT2014. The hydrogen atoms were refined isotropically, and the heavy atoms were refined anisotropically. N-H and O-H hydrogens were located from different electron density maps, and C-H hydrogens were placed in calculated positions and refined with a riding model. Data were corrected for the effects of absorption using SADABS4 Relevant crystal data and refinement results are summarized in Table S1

Table S1. Crystal data and structure refinement for **5**, **7**, **8/4**, **10**•H_2O and **11**•$3H_2O$**.**

Crystal	**5**	**7**	**8/4**
CCDC number	1909774	1918708	1918709
Empirical formula	C_6H_9 Cl N_8O_2	C_6H_9 Cl N_8O_6	$C_{12}H_{17}N_{19}O_8$
Formula weight	260.66	324.66	555.44
Temperature	100.0 K	100.0 K	100.0 K
Crystal system	monoclinic	monoclinic	triclinic
Space group	$P2_1/n$	$P2_1/c$	P-1
a [Å]	6.8258(2) Å	15.9751(9) Å	9.7415(8) Å
b [Å]	23.6441(9) Å	5.4951(3) Å	10.0524(7) Å
c [Å]	7.0643(2) Å	14.4991(9) Å	12.6642(10) Å
α [°]	90°	90°	85.927(2)°
β [°]	108.5760(10)°	103.913(2)°	77.591(2)°
γ [°]	90°	90°	69.175(2)°
Volume	1080.71(6)Å^3	1235.46(12) Å^3	1132.03(15)Å^3
Z	4	4	2
ρ(g cm^{-3})	1.602	1.745	1.630
F(000)	536.0	664.0	572.0

Crystal size (mm^3)	0.28 × 0.15 × 0.12	0.4 × 0.08 × 0.05	0.15 × 0.12 × 0.08
Theta range for data collection	6.324° to 55.002°	5.254° to 55.034°	4.57° to 52.818°
Index ranges	-8 ⩽ h ⩽ 8, -30 ⩽ k ⩽ 30, -9 ⩽ l ⩽ 9	-20 ⩽ h ⩽ 20, -7 ⩽ k ⩽ 6, -18 ⩽ l ⩽ 18	R_{int} = 0
Reflections collected	12802	14034	4613
Independent reflections	2473	2821	4613
Goodness-of-fit on F^2	1.169	1.077	1.050
Final R indices [I>2σ(I)]	R_1 = 0.0524, wR_2 = 0.0908	R_1 = 0.0338, wR_2 = 0.0719	R_1 = 0.0511, wR_2 = 0.1089
R indices (all data)	R_1 = 0.0715, wR_2 = 0.0976	R_1 = 0.0415, wR_2 = 0.0759	R_1 = 0.0887, wR_2 = 0.1226

Table S1. Continued

Crystal	**10**•H_2O	**11**•$3H_2O$
CCDC number	1909777	1918707
Empirical formula	$C_5H_8N_8O_3$	$C_5H_{15}N_9O_5$
Formula weight	228.19	281.26
Temperature	173.0 K	100.0 K
Crystal system	monoclinic	monoclinic
Space group	$P2_1/c$	P21/n
a [Å]	12.4819(13) Å	7.765(3) Å
b [Å]	5.2281(5) Å	7.205(3) Å
c [Å]	14.6301(19) Å	23.573(10) Å
α [°]	90°	90°

β [°]	94.637(4)°	94.770(15)°
γ [°]	90°	90°
Volume	951.59(18) Å^3	1314.3(10) Å^3
Z	4	4
ρ(g cm^{-3})	1.593	1.421
F(000)	472.0	592.0
Crystal size (mm^3)	0.35 × 0.06 × 0.04	0.15 × 0.12 × 0.08
Theta range for data collection	6.244° to 50.848°	5.404° to 54.738°
Index ranges	-15 ⩽ h ⩽ 15, -6 ⩽ k ⩽ 6, -13 ⩽ l ⩽ 17	-9 ⩽ h ⩽ 9, -9 ⩽ k ⩽ 9, -30 ⩽ l ⩽ 26
Reflections collected	4783	11228
Independent reflections	1736	2805
Goodness-of-fit on F^2	1.022	1.053
Final R indices [I>2σ(I)]	R_1 = 0.0578, wR_2 = 0.1130	R1 = 0.0430, wR2 = 0.0865
R indices (all data)	R1 = 0.1259, wR2 = 0.1398	R_1 = 0.0718, wR_2 = 0.1005

Table S2. Hydrogen bonds present in **5**.

D—H…A	d(D-H)/ Å	d(H...A)/ Å	d(D...A)/ Å	<(DHA)/ °	Symmetry code
N4—H4…Cl1	0.8800	2.5900	3.150(2)	122.00	x,y,-1+z
N4—H4…O1	0.8800	2.4800	3.173(3)	136.00	-1+x,y,-1+z
N6—H6A…Cl1	0.87(2)	2.43(2)	3.265(2)	161(2)	-1+x,y,-1+z

N6—H6B…Cl1	0.88(3)	2.51(2)	3.300(2)	149(3)	-x,1-y,1-z
N7—H7…Cl1	0.8800	2.1600	3.013(2)	162.00	/

Table S3. Hydrogen bonds present in **7**.

D—H…A	d(D-H)/ Å	d(H...A)/ Å	d(D...A)/ Å	<(DHA)/ °	Symmetry code
N1—H1A…O2	0.87(2)	2.39(2)	2.920(2)	119.2(19)	1-x, 1-y, 1-z
N1—H1A…O1	0.87(2)	2.27(2)	3.077(2)	153(2)	x, -1/2-y, -1/2+z
N1—H1B…O4	0.87(2)	2.40(2)	3.216(2)	156(2)	1-x, -y, 1-z
N4—H4…O6	0.86(2)	1.94(2)	2.7749(19)	162(2)	-x, -1/2-y, 1/2-z
N5—H5…O4	0.81(2)	2.19(2)	2.960(2)	158(2)	x, 1+y, z

Table S4. Hydrogen bonds present in **8/4**.

D—H…A	d(D-H)/ Å	d(H...A)/ Å	d(D...A)/ Å	<(DHA)/ °	Symmetry code
N7—H7…O4	0.8800	2.2100	3.030(3)	156.00	1-x,1-y,2-z
N9—H9A…O6	0.88(2)	2.37(2)	3.188(3)	155(2)	1-x,1-y,1-z
N9—H9B…O6	0.87(2)	2.19(2)	2.931(3)	143(3)	x,-1+y,1+z
N9—H9B…O7	0.87(2)	2.22(3)	2.979(3)	146(2)	x,-1+y,1+z
N12—H12…N10	0.95(3)	1.83(3)	2.765(3)	170(3)	/
N15— H15A…O5	0.85(2)	2.22(2)	3.055(3)	166(2)	/
N15— H15B… N11	0.86(2)	2.14(2)	2.980(3)	164(2)	2-x,1-y,1-z
N16— H16…O2	0.8800	1.9900	2.833(2)	159.00	1-x,2-y,1-z

Table S5. Hydrogen bonds present in **10**•H_2O.

D—H…A	d(D-H)/ Å	d(H...A)/ Å	d(D...A)/ Å	<(DHA)/ °	Symmetry code
O3—H3D…O2	0.77(4)	2.12(4)	2.877(4)	167(4)	2-x,1-y,1-z
O3—H3E…O3	0.98(7)	2.08(6)	3.038(4)	166(5)	2-x,1/2+y,3/2-z
N4—H4A…N5	0.91(4)	1.98(4)	2.882(4)	172(4)	1-x,1/2+y,3/2-z
N8—H8 …O3	0.90(4)	2.00(4)	2.804(4)	147(3)	/

Table S6. Hydrogen bonds present in **11**•$3H_2O$.

D—H…A	d(D-H)/ Å	d(H...A)/ Å	d(D...A)/ Å	<(DHA)/ °	Symmetry code
O1—H1A…O2	0.89(2)	1.96(2)	2.836(2)	168(2)	/
O1—H1B…N2	0.89(2)	1.87(2)	2.751(2)	171.7(19)	x,1+y,z
O2—H2A…N3	0.88(2)	2.10(2)	2.965(2)	168(2)	3/2-x,1/2+y,3/2-z
O2—H2B…O3	0.87(2)	1.99(2)	2.855(2)	170(2)	/
O3—H3A…N2	0.87(2)	2.57(2)	3.290(2)	142(2)	x,1+y,z

O3—H3B…N4	0.89(2)	1.94(2)	2.802(2)	164(3)	/
N5—H5 …N1	0.8800	2.0700	2.932(2)	168.00	1-x,-y,1-z
N9—H9A…O1	0.94(2)	1.93(2)	2.859(2)	174(2)	/
N9—H9B…O3	0.94(2)	2.03(2)	2.906(3)	154(2)	-1+x,y,z
N9—H9B…O5	0.94(2)	2.60(2)	3.062(3)	110.9(16)	1-x,2-y,1-z
N9—H9C…O1	0.92(2)	2.04(2)	2.956(2)	175(2)	1/2-x,-1/2+y,3/2-z
N9—H9D…O2	0.93(2)	2.05(2)	2.944(2)	159(2)	1/2-x,1/2+y,3/2-z

3 Theoretical Study

Theoretical calculations were performed by using the Gaussian 09 (Revision D.01) suite of programs.[1] The elementary geometric optimization and the frequency analysis were performed at the level of the Becke three parameter, Lee-Yan-Parr (B3LYP)[9] functional with the 6-311+G** basis set.[2] All of the optimized structures were characterized to be local energy minima on the potential surface without any imaginary frequencies. Atomization energies were calculated by the CBS-4M.[3] All the optimized structures were characterized to be true local energy minima on the potential-energy surface without imaginary frequencies.[4]

The predictions of heat of formation (*HOF*) adopt the hybrid DFT-B3LYP methods with 6-311+G** basis set via designed isodesmic reactions. The isodesmic reaction processes, i.e., the number of each kind of formal bond is conserved, are used with application of the bond separation reaction (BSR) rules. The molecule is broken down into a set of two heavy-atom molecules containing the same component bonds. The isodesmic reactions used to derive the HOF of the title compounds are in Scheme S1. The change of enthalpy for the reactions at 298 K can be expressed as

$$\Delta H_{298} = \sum \Delta_f H_P - \sum \Delta_f H_R \quad (1)$$

Where $\sum \Delta_f H_P$ and $\sum \Delta_f H_R$ are the *HOF* of reactants and products at 298 K, respectively, and ΔH_{298} can be calculated using the following expression:

$$\Delta H_{298} = \Delta E_{298} + \Delta(PV) = \Delta E_0 + \Delta ZPE + \Delta H_T + \Delta nRT \quad (2)$$

Where ΔE_0 is the change in total energy between the products and the reactants at 0 K; ΔZPE is the difference between the zero-point energies (*ZPE*) of the products and the reactants at 0 K; ΔH_T is thermal correction from 0 to 298 K. The $\Delta(PV)$ value in eq (2) is the *PV* work term. It equals $\Delta(nRT)$ for the reactions of ideal gas. For the isodesmic reaction, $\Delta n = 0$, so $\Delta(PV) = 0$. On the left side of Eq. (1), apart from target compound, all the others are called reference compounds. The HOF of reference compounds is available from the experiments.

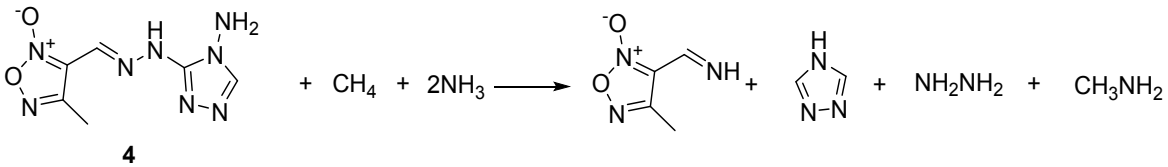

4

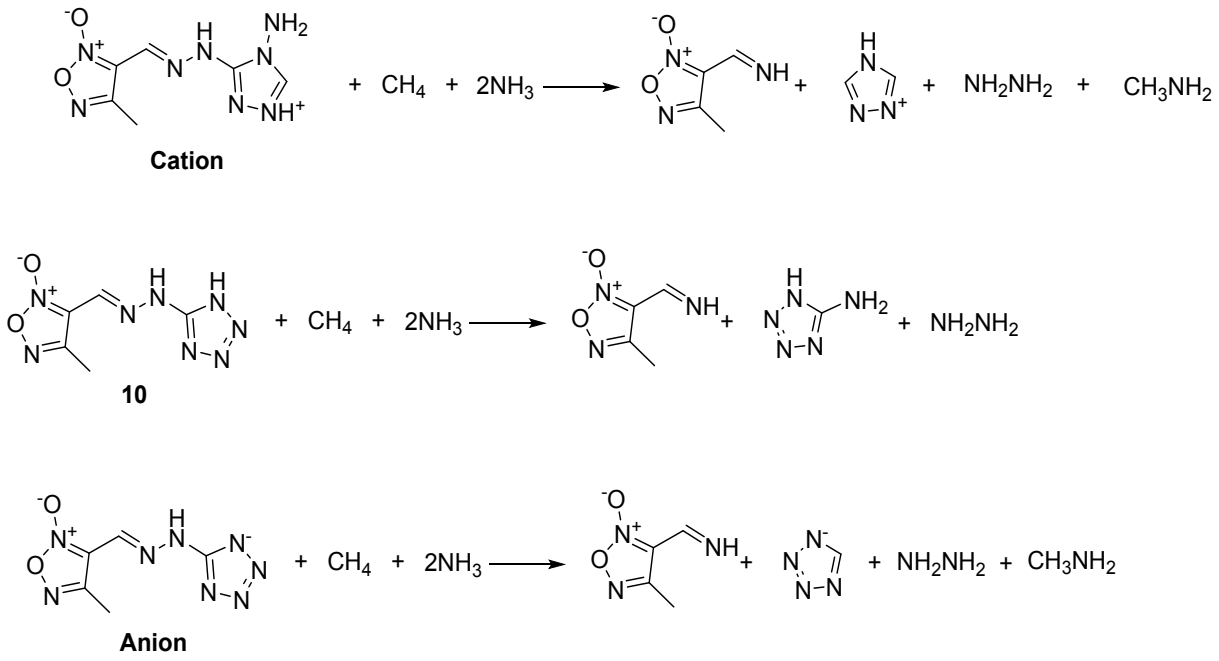

Scheme S1. Isodesmic reactions of target compounds.

Table S7 Ab initio computational values of small molecules used in isodesmic and tautomeric reactions.

Compound	E_0[a]	ZPE[b]	H_T[c]	HOF[d]
NH_2NH_2	-111.91	134.28	11.16	95.4
CH_3NH_2	-95.89	160.78	11.64	-22.5
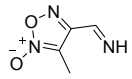	-470.11	248.22	25.28	257.97
	-257.79	84.91	11.26	175.75
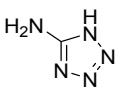	-313.71	329.91	20.78	330.60
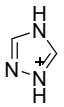	-242.7	184.01	12.27	841.25
	-242.32	150.39	12.06	192.7

[a]Total energy calculated by B3LYP/6-311+G**method (a.u);[b]zero-point correction (kJ mol^{-1}); [c] thermal correction to enthalpy (kJ mol^{-1}); [d] heat of formation (kJ mol^{-1}).

4 Reference

[1] Frisch, M. J.; Trucks, G. W.; Schlegel, H. B.; Daniels, A. D.; Farkas, O.; Foresman, J. B.; Ortiz, J. V.; Cioslowski, J.; Fox, D. J. Gaussian 09, Revision D. 01, Gaussian. Inc. Wallingford CT, **2009**.

[2] P. C. Hariharan, J. A. Pople, Theor. Chim. Acta. 1973, 28, 213-222.

[3] J. W. Ochterski, G. A. Petersson, J. A. Montgomery, J. Chem. Phys. 1996, 104, 2598-2619.

[4] H. D. B. Jenkins, D. Tudeal, L. Glasser, Inorg. Chem. 2002, 41, 2364-2367.

5 ^{1}H and ^{13}C NMR Spectra of Compounds

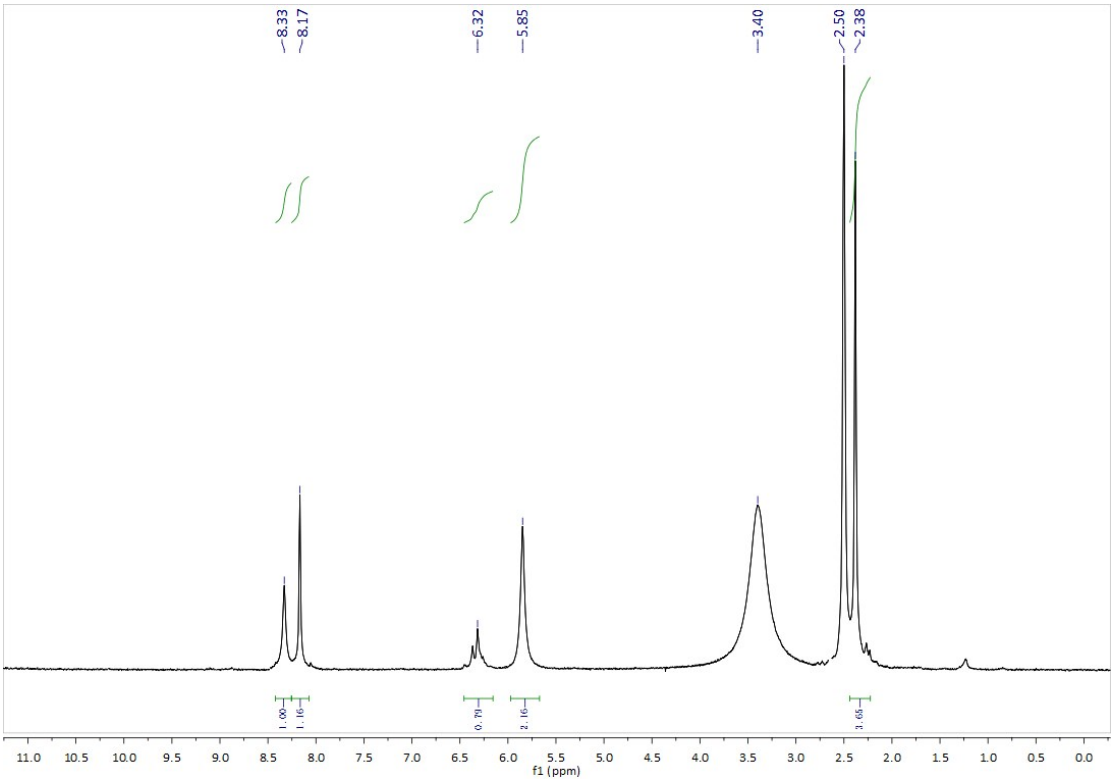

Figure S1 ^{1}H NMR spectra (500 MHz) of **4** in [D_6] DMSO at 25 ^{o}C.

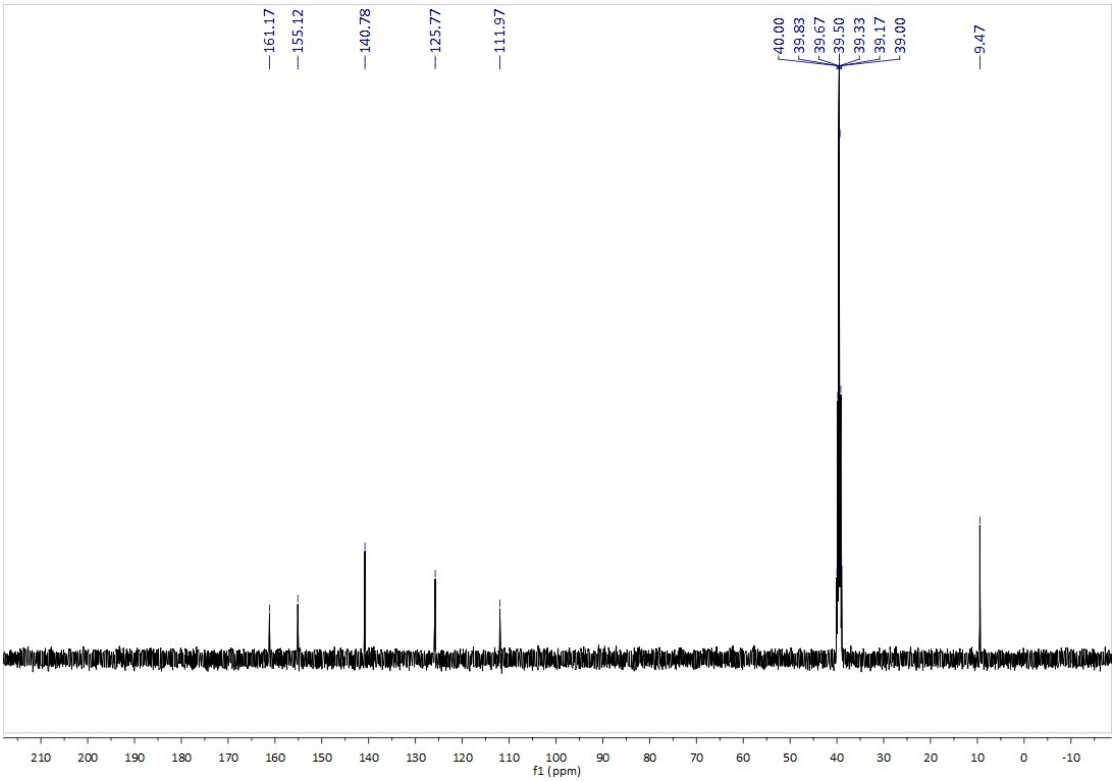

Figure S2 ^{13}C NMR spectra (125 MHz) of **4** in [D_6] DMSO at 25 ^{o}C.

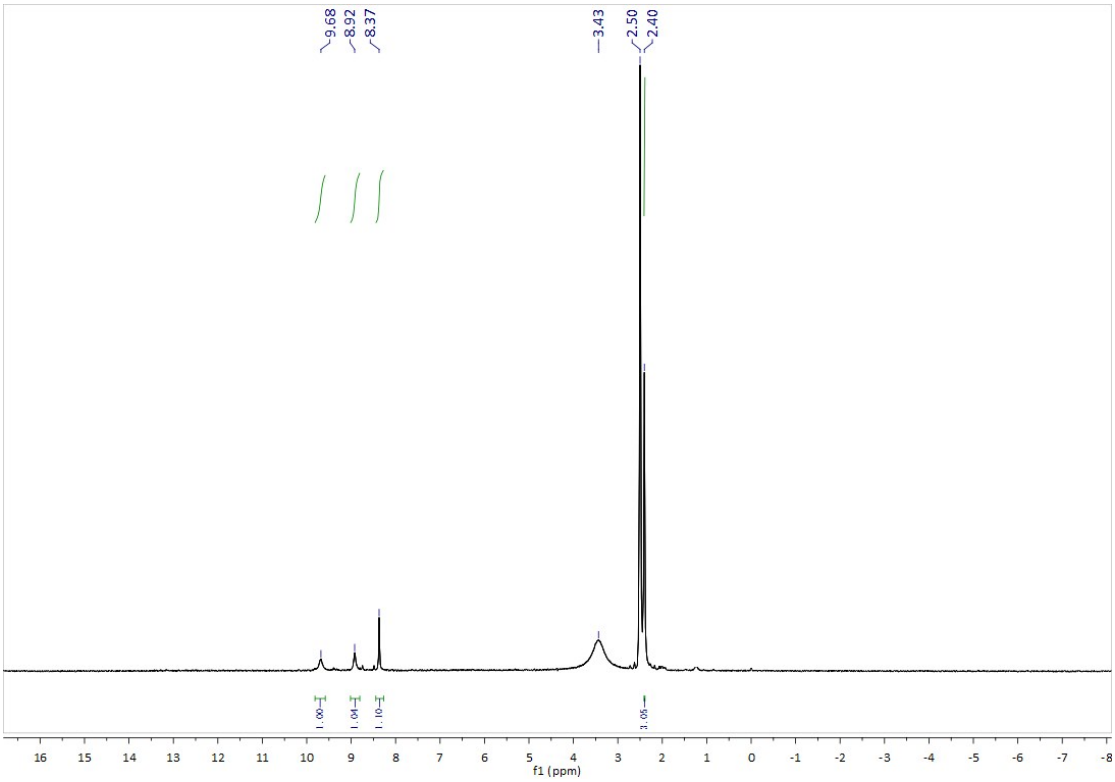

Figure S3 ^{1}H NMR spectra (500 MHz) of **6** in [D_6] DMSO at 25 ^{o}C.

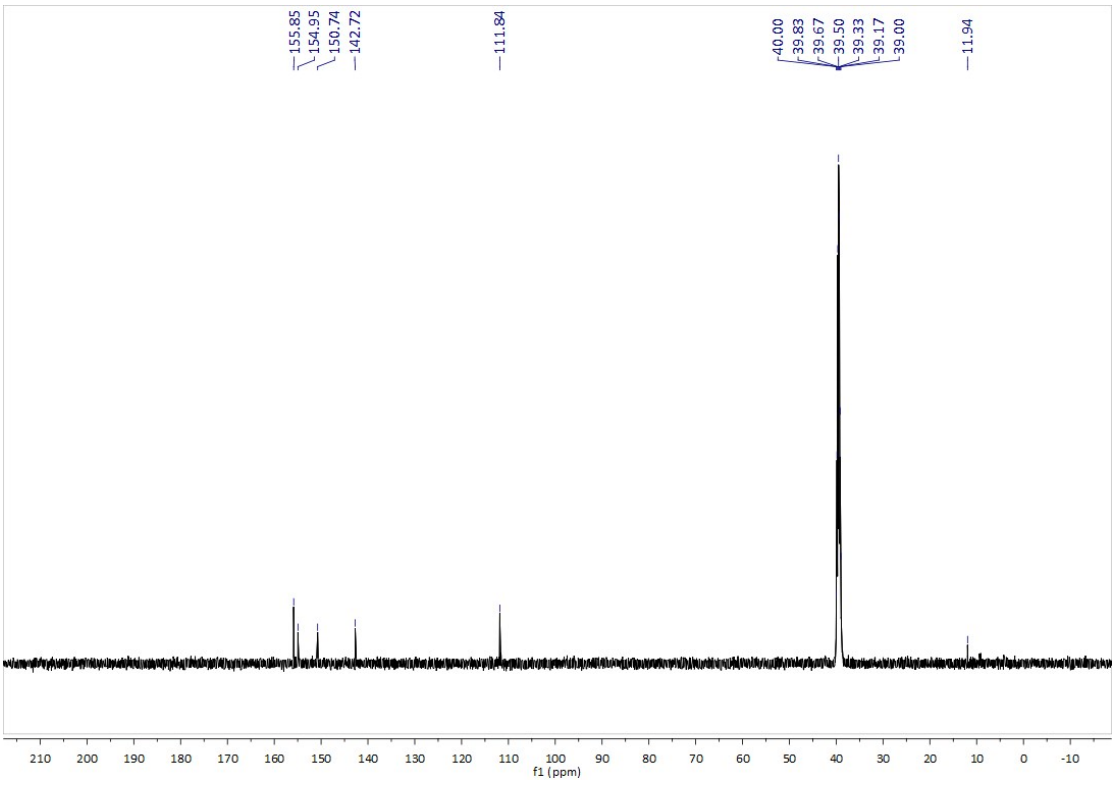

Figure S4 ^{13}C NMR spectra (125 MHz) of **6** in [D_6] DMSO at 25 ^{o}C.

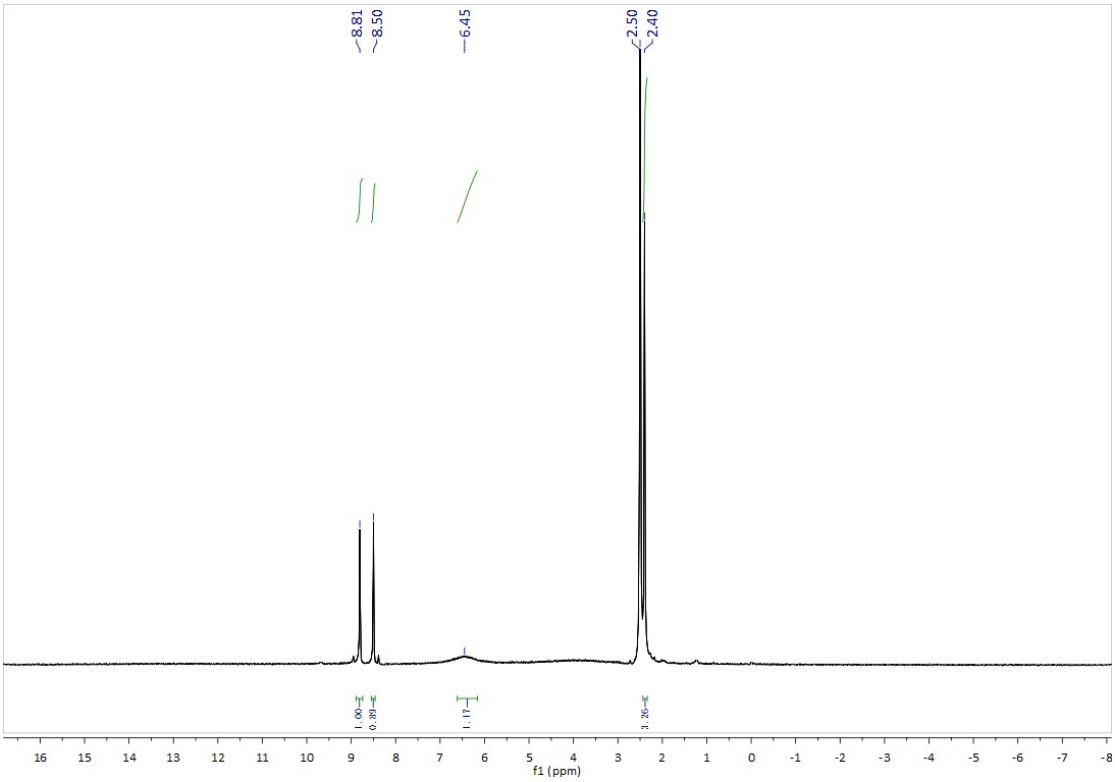

Figure S5 ^{1}H NMR spectra (500 MHz) of **7** in [D_6] DMSO at 25 ^{o}C.

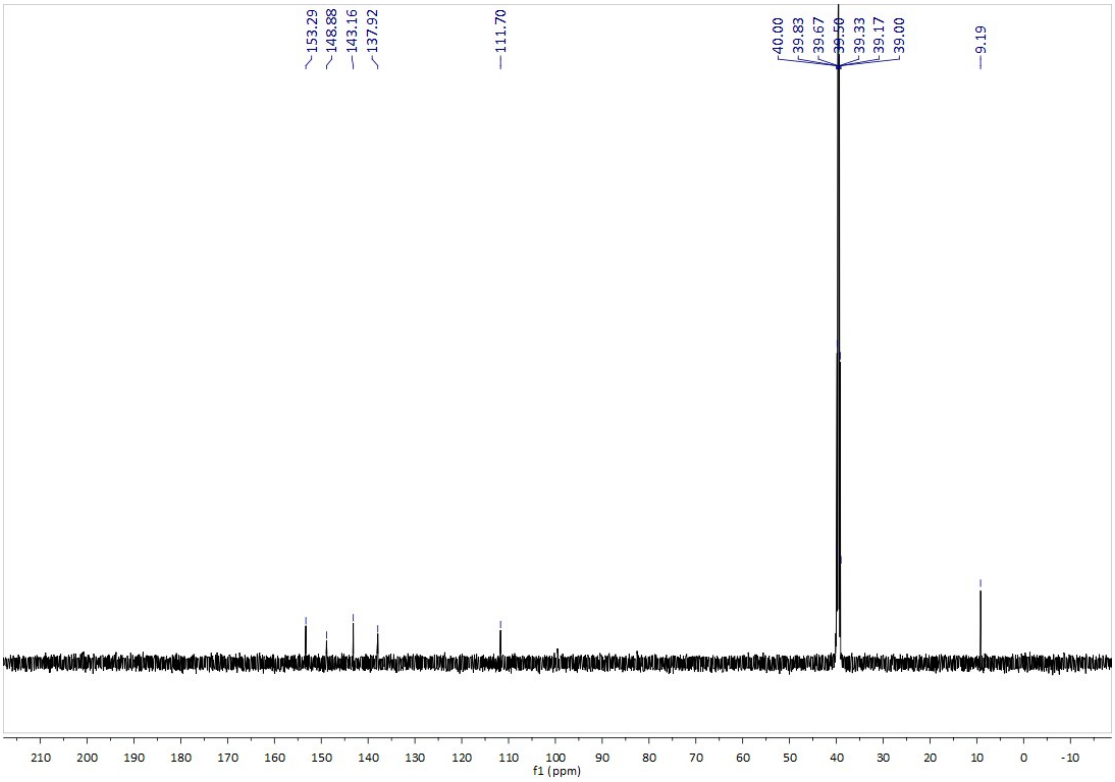

Figure S6 ^{13}C NMR spectra (125 MHz) of **7** in [D_6] DMSO at 25 ^{o}C.

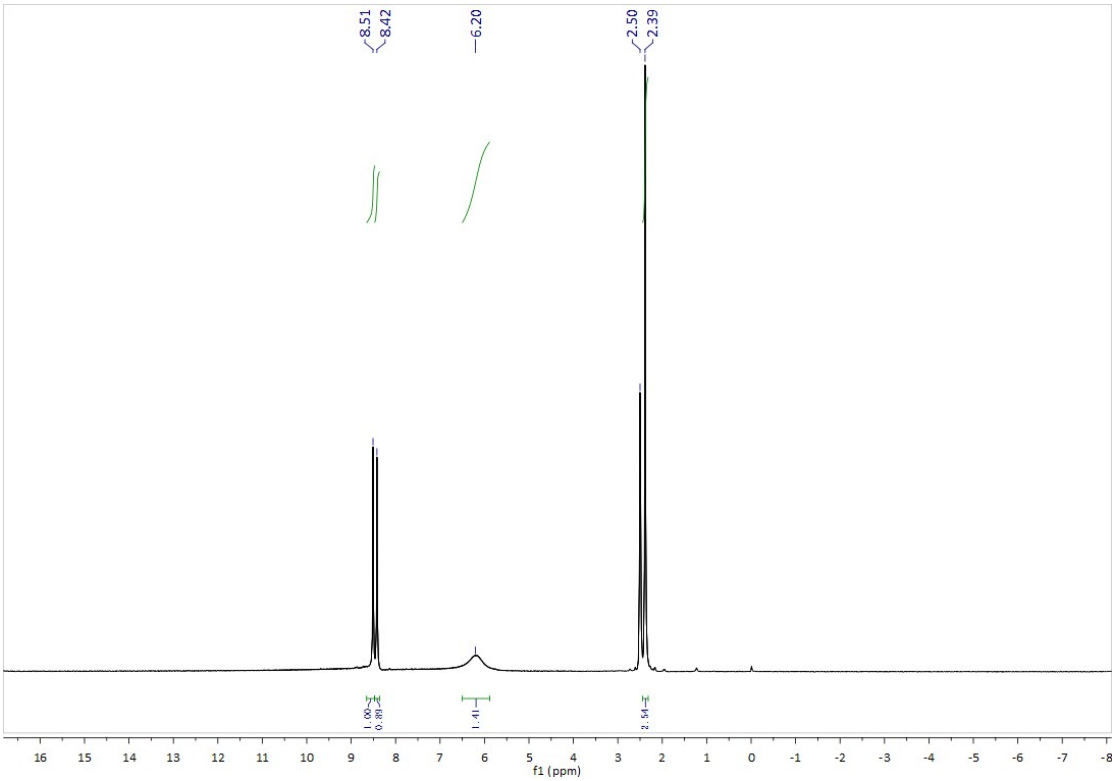

Figure S7 ^{1}H NMR spectra (500 MHz) of **8** in [D_6] DMSO at 25 ^{o}C.

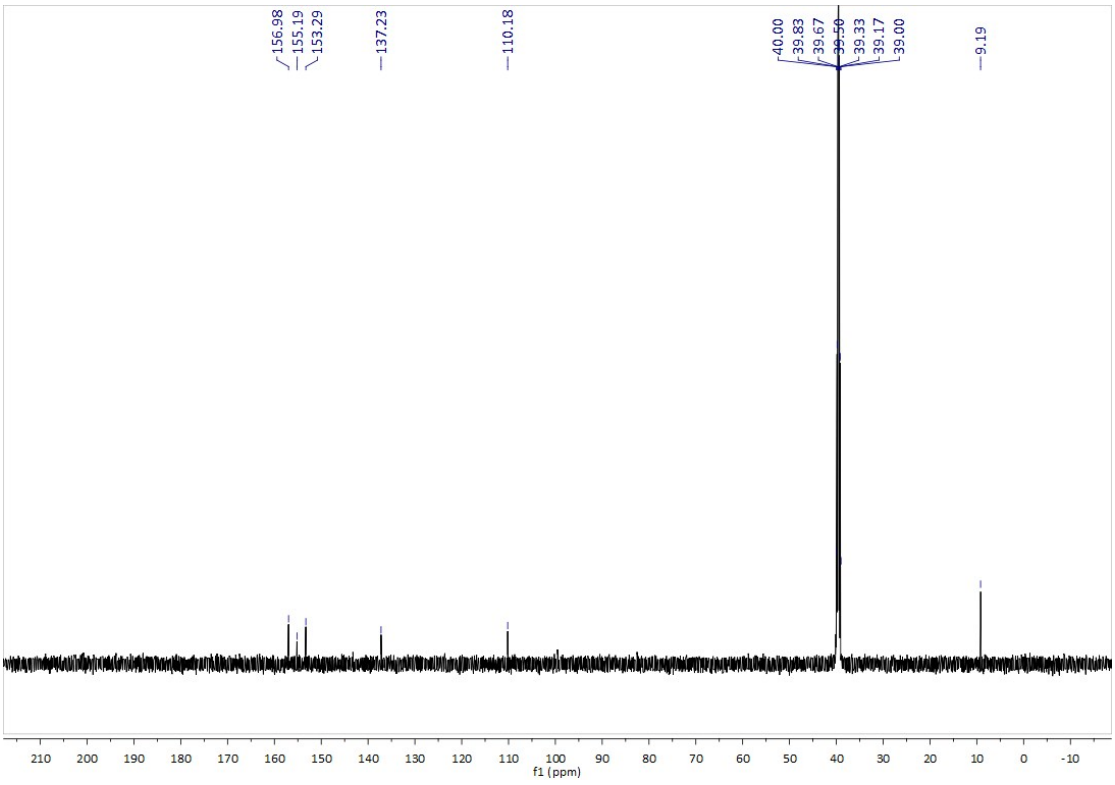

Figure S8 ^{13}C NMR spectra (125 MHz) of **8** in [D_6] DMSO at 25 ^{o}C.

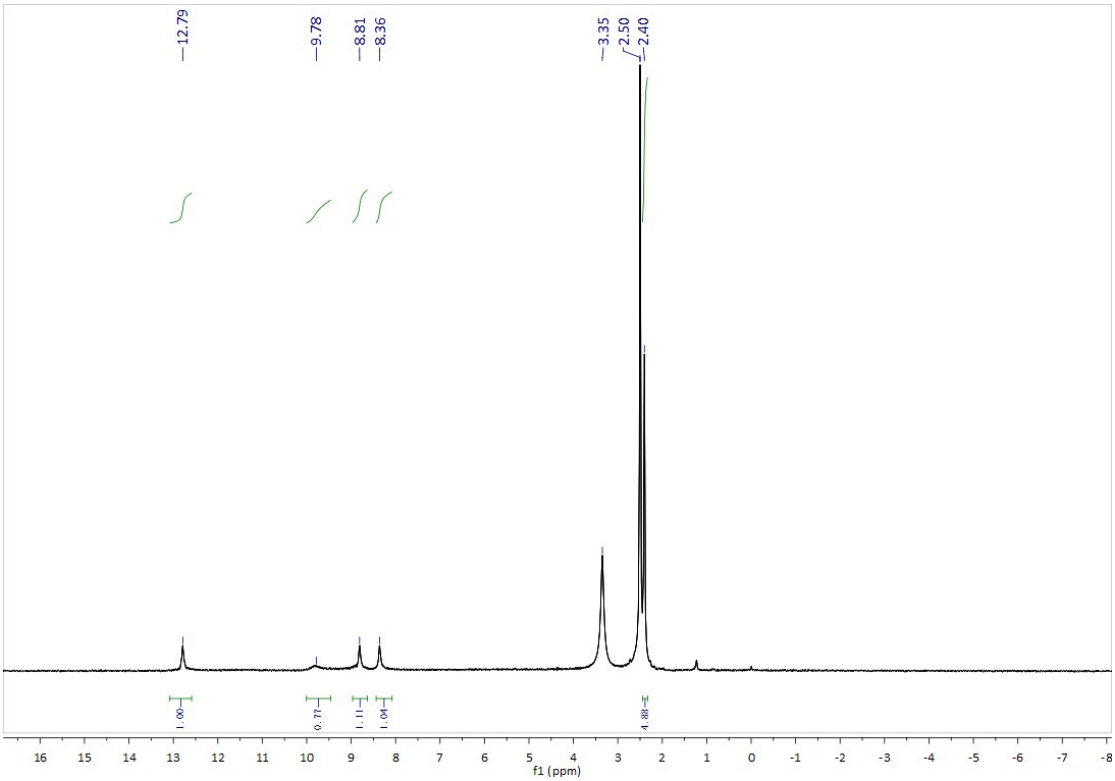

Figure S9 ^{1}H NMR spectra (500 MHz) of **9** in [D_6] DMSO at 25 ^{o}C.

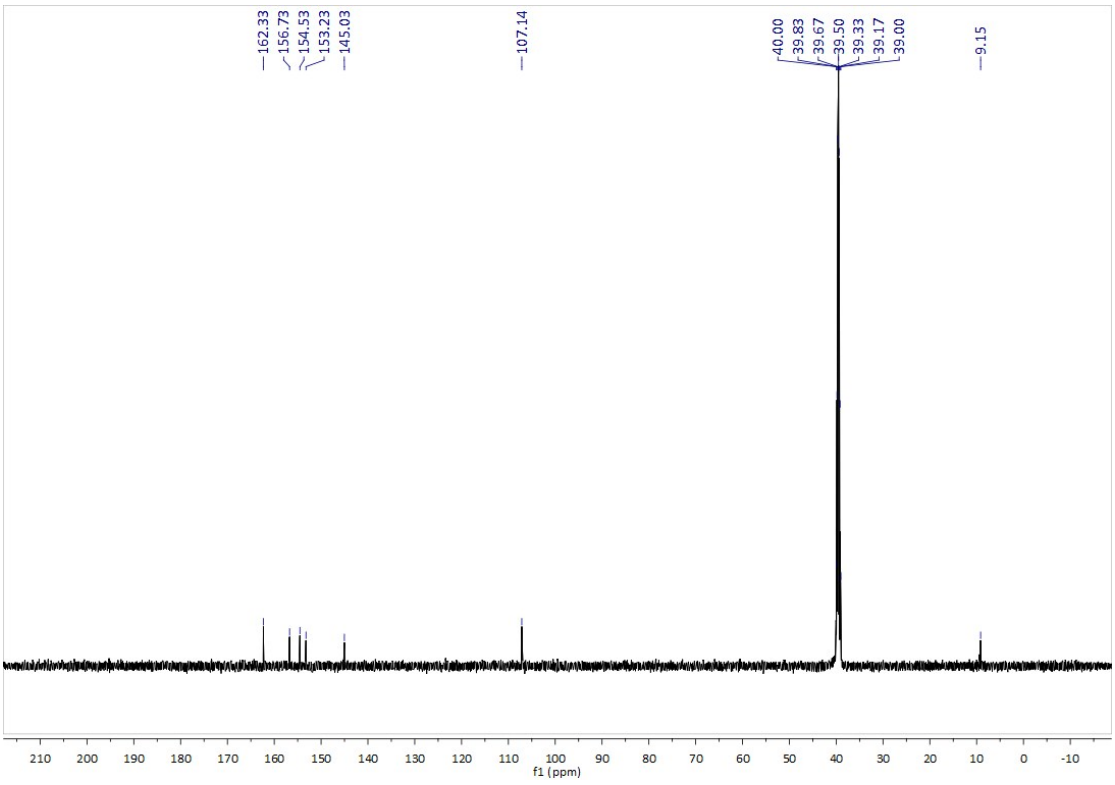

Figure S10 ^{13}C NMR spectra (125 MHz) of **9** in [D_6] DMSO at 25 ^{o}C.

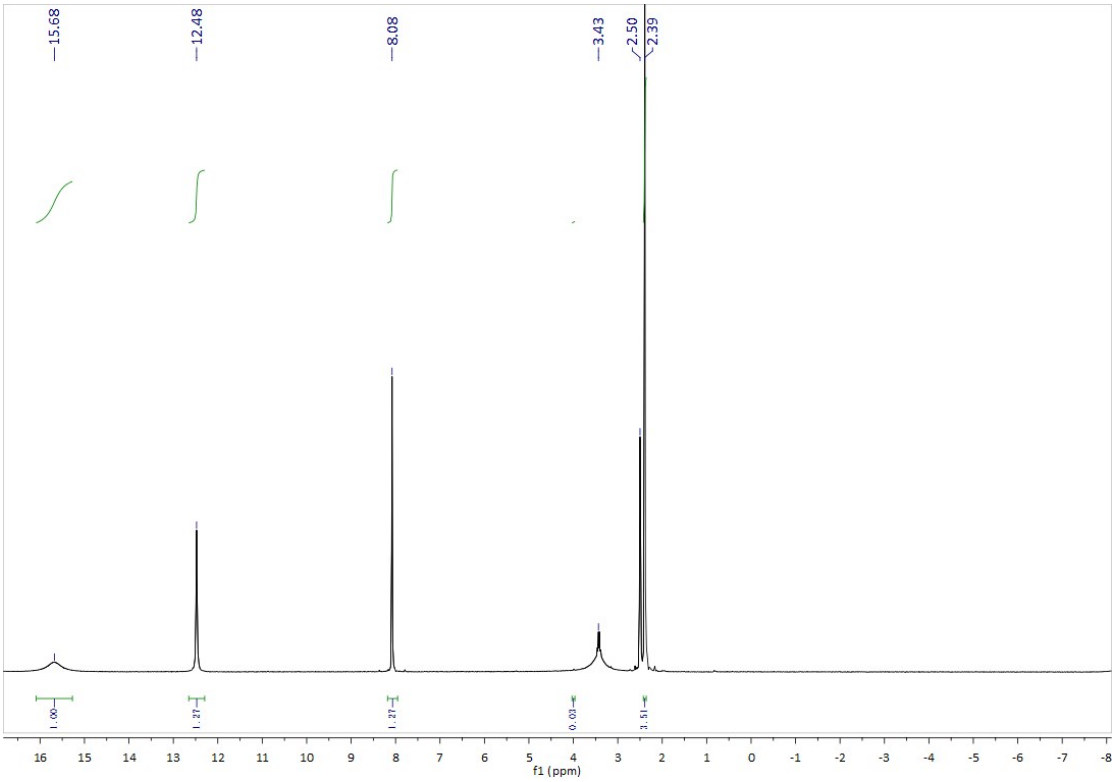

Figure S11 ^{1}H NMR spectra (500 MHz) of **10** in [D_6] DMSO at 25 ^{o}C.

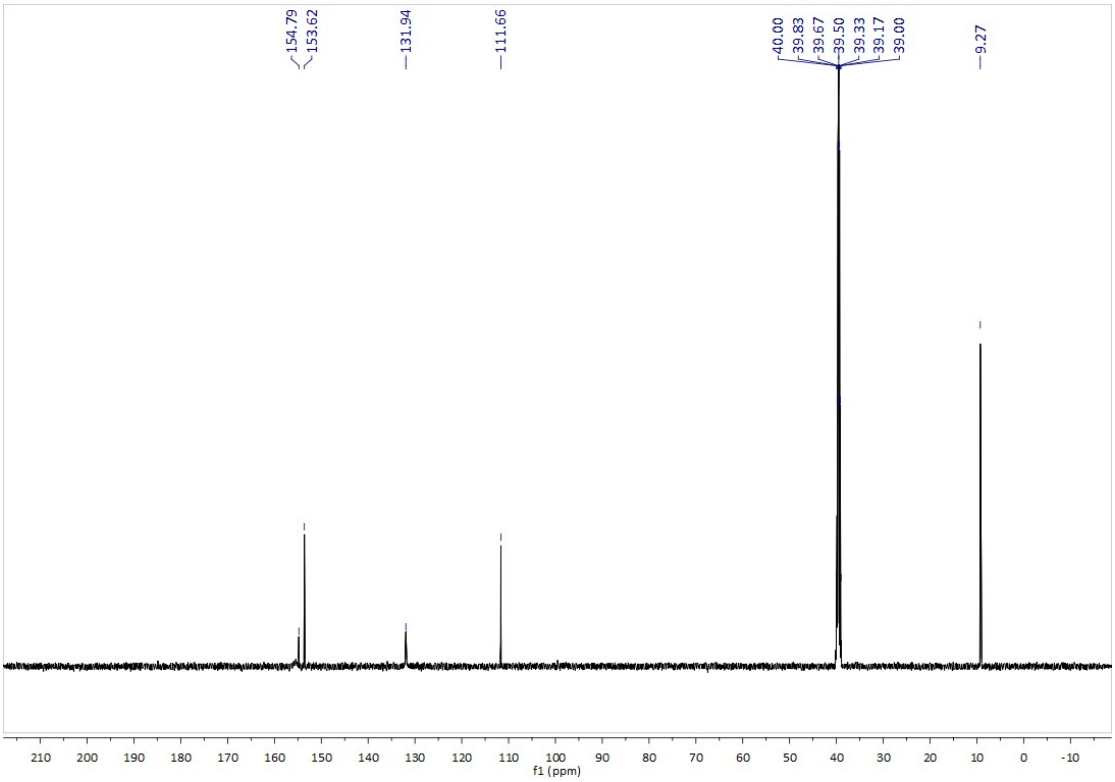

Figure S12 ^{13}C NMR spectra (125 MHz) of **10** in [D_6] DMSO at 25 ^{o}C.

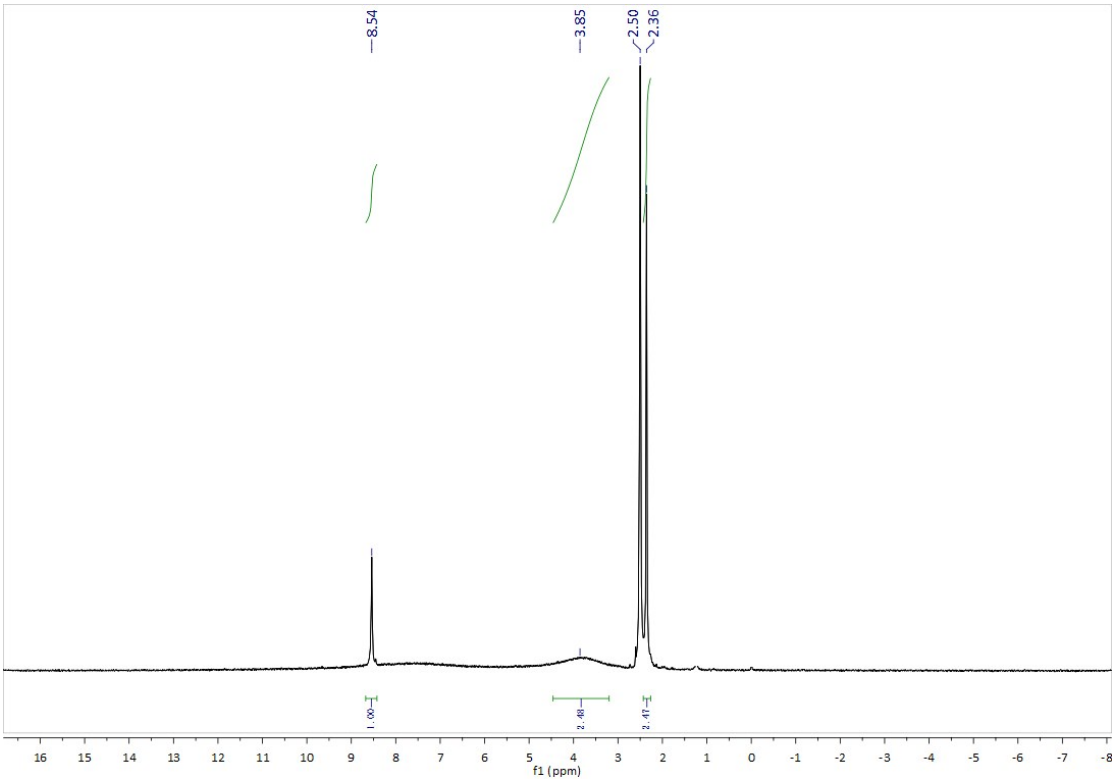

Figure S13 ^{1}H NMR spectra (500 MHz) of **11** in [D_6] DMSO at 25 ^{o}C.

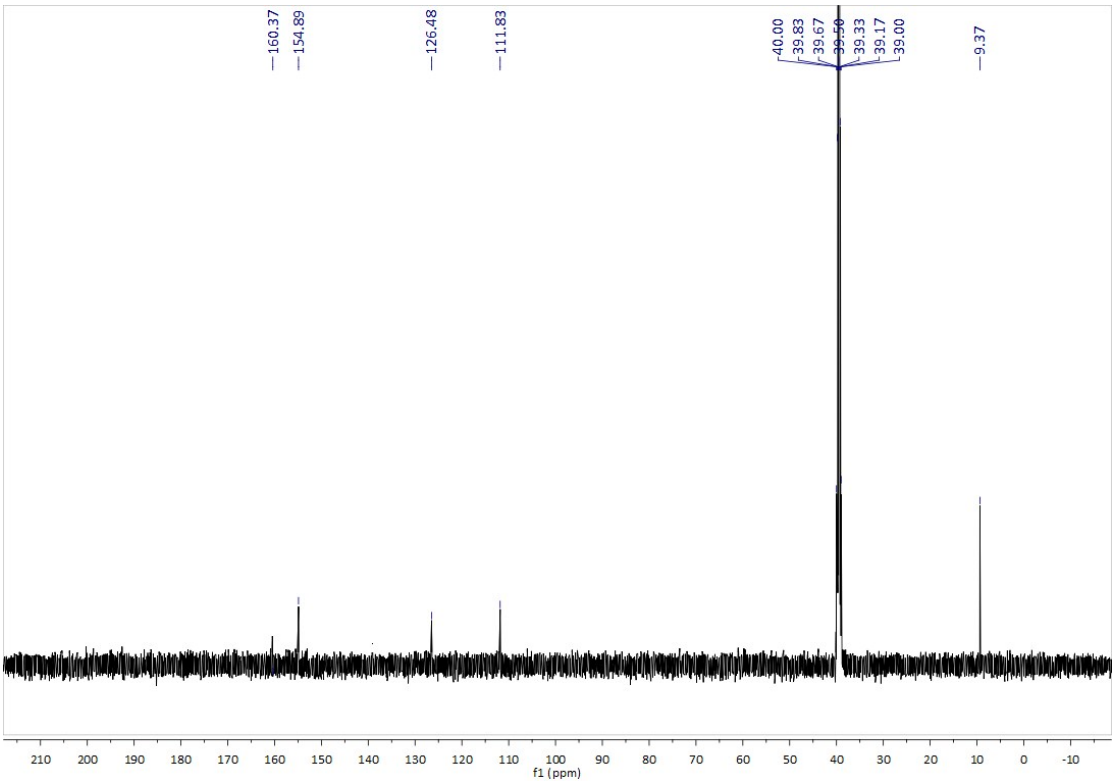

Figure S14 ^{13}C NMR spectra (125 MHz) of **11** in [D_6] DMSO at 25 ^{o}C.

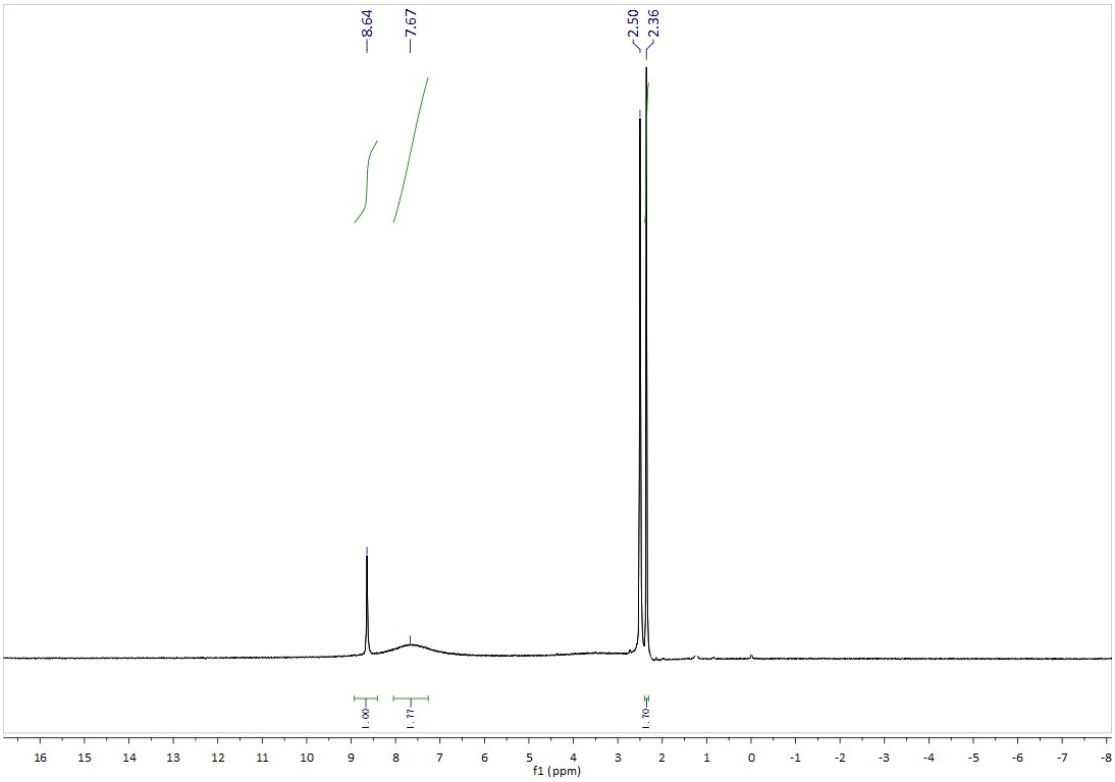

Figure S15 ^{1}H NMR spectra (500 MHz) of **12** in [D_6] DMSO at 25 ^{o}C.

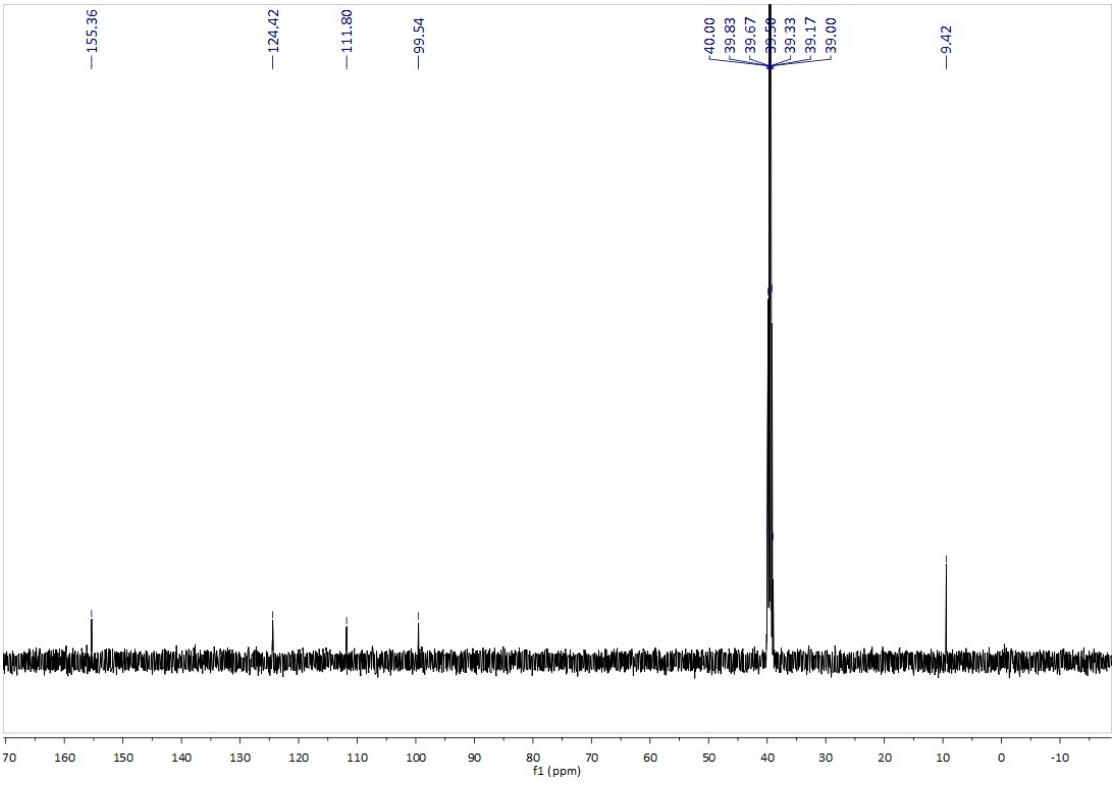

Figure S16 ^{13}C NMR spectra (125 MHz) of **12** in [D_6] DMSO at 25 ^{o}C.

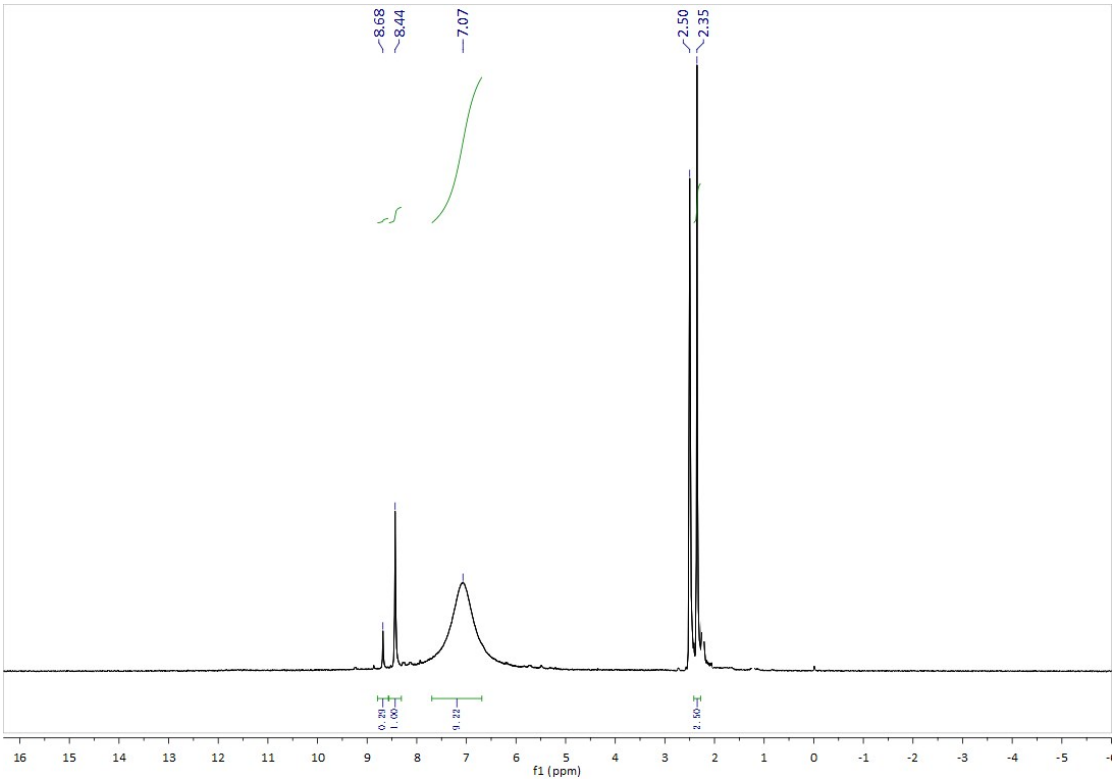

Figure S17 ^{1}H NMR spectra (500 MHz) of **13** in [D_6] DMSO at 25 ^{o}C.

Figure S18 ^{13}C NMR spectra (125 MHz) of **13** in [D_6] DMSO at 25 ^{o}C.

6 Thermal behavior of cocrystal 8/4

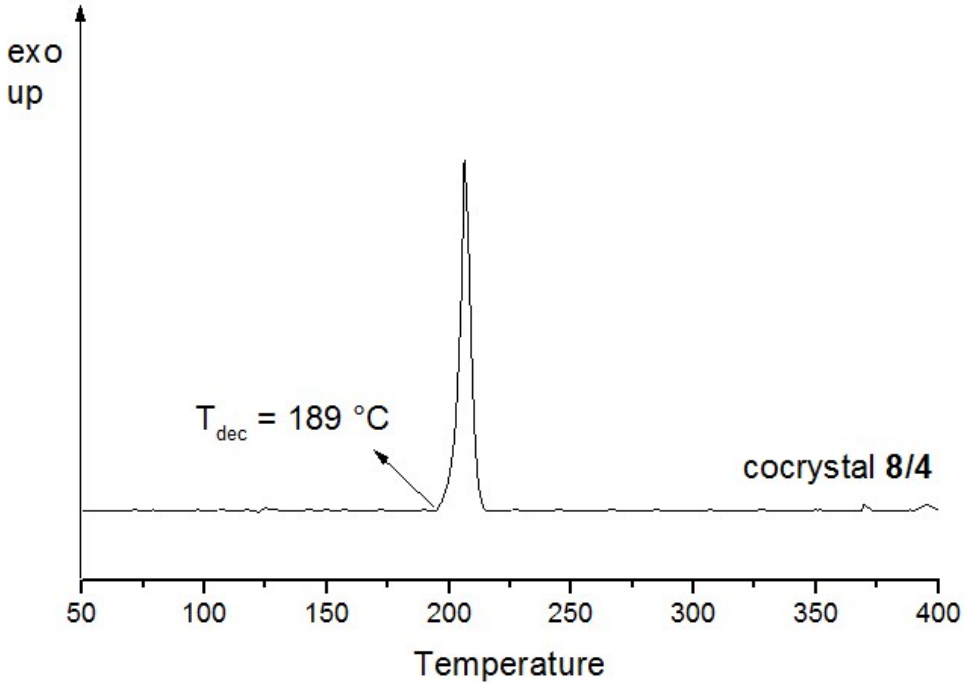

Figure S19 DSC plot of cocrystal **8/4.**